World Academy of Science, Engineering and Technology
International Journal of Aerospace and Mechanical Engineering
Vol:8, No:5, 2014

Conceptual Design of the *TransAtlantic* as a Research Platform for the Development of "Green" Aircraft Technologies

Victor Maldonado

Abstract—Recent concerns of the growing impact of aviation on climate change has prompted the emergence of a field referred to as Sustainable or "Green" Aviation dedicated to mitigating the harmful impact of aviation related CO_2 emissions and noise pollution on the environment. In the current paper, a unique "green" business jet aircraft called the *TransAtlantic* was designed (using analytical formulation common in conceptual design) in order to show the feasibility for transatlantic passenger air travel with an aircraft weighing less than 10,000 pounds takeoff weight. Such an advance in fuel efficiency will require development and integration of advanced and emerging aerospace technologies. The TransAtlantic design is intended to serve as a research platform for the development of technologies such as *active flow control*. Recent advances in the field of active flow control and how this technology can be integrated on a sub-scale flight demonstrator are discussed in this paper. Flow control is a technique to modify the behavior of coherent structures in wall-bounded flows (over aerodynamic surfaces such as wings and turbine nozzles) resulting in improved aerodynamic cruise and flight control efficiency. One of the key challenges to application in manned aircraft is development of a robust high-momentum actuator that can penetrate the boundary layer flowing over aerodynamic surfaces. These deficiencies may be overcome in the current development and testing of a novel *electromagnetic synthetic jet* actuator which replaces piezoelectric materials as the driving diaphragm. One of the overarching goals of the TranAtlantic research platform include fostering national and international collaboration to demonstrate (in numerical and experimental models) reduced CO_2/ noise pollution via development and integration of technologies and methodologies in design optimization, fluid dynamics, structures/ composites, propulsion, and controls.

Keywords—Aircraft Design, Sustainable "Green" Aviation, Active Flow Control, Aerodynamics.

I. Introduction

THE aviation industry contributes about 2-3% of the global man-made CO_2 emissions and supports an estimated 3.2% of worldwide economic activity in terms of GDP (2007 figure) [1]. In 2008, the U.S. spent a total of $73 billion in jet fuel, which represents approximately 40% of airlines' operating costs [2], [3]. Meanwhile, there is a projected growth in commercial air travel from 704 million U.S. travelers in 2009 to 1.21 billion by 2030 [3]. With rising demand for passenger air travel, aviation has become the fastest growing form of CO_2 producer in the transportation sector. These alarming statistics have helped mobilize the scientific community to study the current impact of aviation practices on climate change and local air quality, and devise methods to mitigate the amount of CO_2 and other harmful byproducts (i.e. NO_2, sulfur, soot) emitted into the atmosphere. These methods can be separated into two main categories; operational or technology driven approaches. Operational approaches are geared towards improving system efficiency, for example reducing the time aircraft spend on departure queues at the taxiway, thereby saving fuel. Technological approaches are more diverse and transformative in reducing aviation's environmental impact. Popular programs include research into more fuel-efficient aircraft designs, propulsion systems (i.e. open-rotor/ propfan concept), nanocomposite structures, and sustainable biofuels which produce lower life-cycle CO_2 emissions.

Victor Maldonado is with the Department of Mechanical Engineering, University of Texas at San Antonio, San Antonio, TX, 78249 USA, (e-mail: victor.maldonado@utsa.edu)

A. Sustainable Aviation Initiatives

In recent years, a number of sustainable aviation initiatives have been formed to address the impact of rapid aviation growth on the environment and society. The European Union, particularly the United Kingdom, has been a leader in recognizing this need and establishing organizations and public/ private partnerships between the aerospace industry and government. For example, *Clean Sky* was formed as an ambitious aeronautical research programme to develop breakthrough technologies to significantly increase the environmental performance of aircraft and air transportation [4]. The organization is managing the Joint Technology Initiative, started in 2008 to develop six integrated technology demonstrators known as: *smart fixed-wing aircraft, green regional aircraft, green rotorcraft, sustainable and green engines, systems for green operations, and eco-design.* The integration of this technology will enable signficiant progress; a reduction in carbon emissions and noise of around 30% from currently operating aircraft systems is envisioned. Most recently in 2013, a *Clean Sky 2* initiave was launched to further meet economic and environmental performance objectives (40% reduction in CO_2 and noise) and noise of new technology through the 2025-2035 timeframe.

The Unites States is also committed to addressing climate change impacts of aviation and operates on the ambitious goal of achieving carbon-neutral growth for U.S. commerical aviation by 2020. Under leadership by the Federal Aviation Administration (FAA) and as outlined in the *Next Generation Air Transportation System Plan* [5], the government has initiatives for improvements in technology and operations,

advances in development of sustainable fuels, and policies to incentivize transition of these systems into airline fleets. This innovation in commercial aviation will be further benefited by the Department of Defense (DoD), which is engaged in similar research for the defense sector. Some environmental performance targets under the FAA Plan include a reduction of 47 million tons (MT) of CO_2 emissions through technology and operations advancements and between 9 and 34 MT from alternative fuels by 2020. Assuming the best case emissions reduction via alternative fuels would still require an additional 34 MT decrease in order to achieve carbon-netrual growth by 2020, assuming the baseline from 2005. The National Aeronautics and Space Administration (NASA) is also playing a crucial role, together with the FAA and DoD, in developing innovative technology for the green aviation effort. NASA is currently involved in research programs (i.e. the Continuous Lower Energy, Emissions and Noise Program and the Environmentally Responsible Aviation Project, [6]) dedicated towards fuel-efficiency improvements in turbine engines and structures.

B. TransAtlantic Green Aircraft Research Platform

The TransAtlantic Green Aircraft Research Platform (T-GARP) is a novel initiative to foster national and international collaboration on green aircraft technologies among academic researchers. At the core of the platform is the TransAtlantic; a unique business jet designed as a feasibility study to achieve unprecedented transatlantic range with an aircraft weighing under 10,000 pounds takeoff weight. The aircraft was conceptually designed using "first-order" analytical formulation. A platform design approach allows the aircraft system to be designed and analyzed at the subsystems level by different researchers, according to area of expertise, and later integrated as a collaborative effort. The four major subsystems comprising the aircraft system are: (i) Configuration and Fluid Dynamics, (ii) Aero-structure, (iii) Propulsion, and (iv) Flight Control. The aircraft configuration and fluid dynamics subsystem is normally considered a lower-level component of the aero-structure, however because there exists the potential to significantly improve the aerodynamics and fuel-efficiency of an aircraft via configuration optimization and flow control techniques, it will be treated as a separate subsystem. Moreover, the author's expertise and research in active flow control allow development of novel techniques and actuators to occur in context as an application to T-GARP and green aviation. More on the application of active flow control on the TransAtlantic and aircraft in general is discussed near the end of the paper.

II. Conceptual Design

The possibility of extending the flight performance of typically sized entry level jets to attain transatlantic non-stop range, i.e. New York City to London (3016 nm) and a cruising speed of Mach 0.78 (comparable to mid-size business jets) is explored with the TransAtlantic. We present in the process the conceptual design of a unique business jet where designing for aerodynamic and operating efficiency is paramount. In the recent literature, there has been many conceptual aircraft designs and methodologies developed by industry and academia for "green" aircraft [7], [8], [9]. The motivation for designing the TransAtlantic jet is two-fold. From a technical perspective, it is a research platform or "test-bed" for the development of green aviation technologies and methods in order to help solve the environmental aviation challenge. From an economic perspective, if the stated performance objectives are met, the aircraft design could reduce the cost per mile by more than 50% and the cost per mile/passenger by an estimated 30% compared to a mid-size business jet (nine to ten passengers, i.e. Gulfstream G200, Learjet 85) traveling the same distance and cruising speed. The TransAtlantic was designed using a combination of analytical formulation found in textbooks such as those from Raymer [10], Corke [11], and Kundu [12].

The overall aircraft design goal is to meet (or exceed) the stated design and mission requirements identified in the beginning of the conceptual design process. In particular the range and cruise Mach number were the driving performance parameters and suggested a design geometry different from what is typically seen on small commuter jets. The key design and mission requirements are the following:

1) Crew: 1 pilot
2) Passenger capacity: 6
3) Takeoff weight: under 10,000 lbs
4) Range: 3,300 nm (transatlantic)
5) Cruise speed/ altitutde: 516 ktas (Mach 0.78) at 40,000 ft

A maximum takeoff weight is typically not a design constraint, rather the aim is to produce the lightest aircraft that can safely perform the mission. The initial conceptual takeoff weight estimate was calculated below 10,000 lbs using fuel fraction estimates based on historical and empirical equations (Brequet range and endurance equations) as well as design variables such as engine thrust, average thrust specific fuel consumption (TSFC), and main wing aspect ratio. These variables were chosen initially based on historical aircraft of similar sized business jets, however they were later refined during the main wing design and engine selection stage. Furthermore, a much more accurate estimate of the takeoff weight (using historical formulas adapted from aircraft manufacturers) is performed once all conceptual design iterations have been made.

A. Aircraft Configuration

A conventional aircraft configuration was selected and included a low on fuselage mounted wing, engines on the aft portion of the fuselage, and a T-tail (horizontal tail on top of vertical tail). This is the most common configuration for small business jets and is desired over unconventional designs because of its aerodynamically clean wing, better engine ground clearance, and improved vertical tail control effectiveness (for engine out trim).

The mission requirements translated into designing for aerodynamic and long range/ high speed cruise efficiency which gave significant insight into the relative size and

geometry of the main aircraft components comprised of the fuselage, main wing, horizontal tail, and vertical tail. The following two major considerations were taken in the design of the TranstatlAntic: (i) a relatively long and narrow fuselage to reduce the "form factor" that takes into account flow separation (pressure drag) above and beyond viscous skin friction drag. (ii) A relatively small high aspect ratio wing (and thus high wing loading) for long range efficiency that minimizes induced drag. The size of the T-tail configuration would then be determined primarily on the size and relative location of the wing on the fuselage, as well as on static/ dynamic stability and control requirements.

B. Wing Design

The main objectives for the wing design included selection of the airfoil which would result in (i) optimal cruising flight performance based on the cruise lift coefficient lying within the drag bucket (a range of minimum drag coefficients) of the airfoil and (ii) the airfoil critical Mach number must be at least slightly higher than the cruise Mach number. Mach 0.78 is at the threshold at which to consider transonic effects and the possible acceleration of local flow to sonic speeds. The second consideration led to the selection of a NASA phase 2 supercritical airfoil, SC(2). Numerical and experimental results of these airfoils are documented in a NASA technical report based on analysis from the 1960s and 1970s [13]. As shown from the plot of Fig. 1, the drag divergence Mach number, M_{DD} decreases linearly as a function of chord thickness. Furthermore for increasing values of design lift coefficient (location of maximum lift to drag ratio, *L/D*), M_{DD} decreases for a given chord thickness. Taking a closer look at the design lift coefficient, this value should ideally be within the range of minimum and maximum cruise trim lift coefficient (a consequence of varying lift generation due to fuel expenditure) because an aircraft achieves its maximum range at the wing's most efficient operation of highest *L/D*.

The business jet's trim lift coefficient at the beginning and end of the cruise phase had been iteratively calculated as 0.41 and 0.25 respectively, with an average value of 0.33. Among the available set of SC(2) airfoils with design lift coefficients of 0.4, 0.7, and 1.0, the closest one to the average of 0.33 is 0.4, which was selected. In order to determine a satisfactory airfoil chord thickness; we impose an M_{DD} value slightly higher than the cruise Mach number. Interpolating from the design lift coefficient of 0.4 curve, we observe that this is satisfied for airfoils with a chord thickness of less than 12%. Selecting from a variety of available airfoil chord thicknesses below 12%, we could conclude that a 10% chord thickness airfoil is ideal; it contains an M_{DD} value of roughly 0.81. In addition, the thicker airfoil (compared to a 6% airfoil which is the next lowest thickness available) provides a higher maximum lift coefficient for takeoff purposes and additional inboard space for wing-mounted fuel tanks and wing flap/aileron actuators.

The plots of Fig. 2 represent numerical results of sonic-plateau pressure distributions for 10% thickness SC(2) airfoils with various design lift coefficient values and the

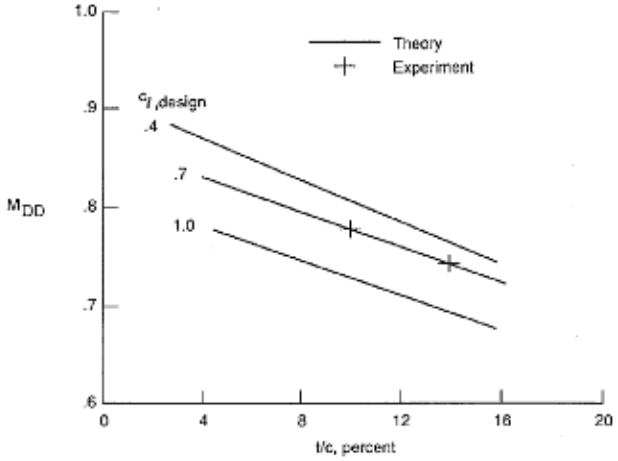

Fig. 1. NASA SC(2) airfoils' drag divergence Mach number vs. percentage chord thickness.

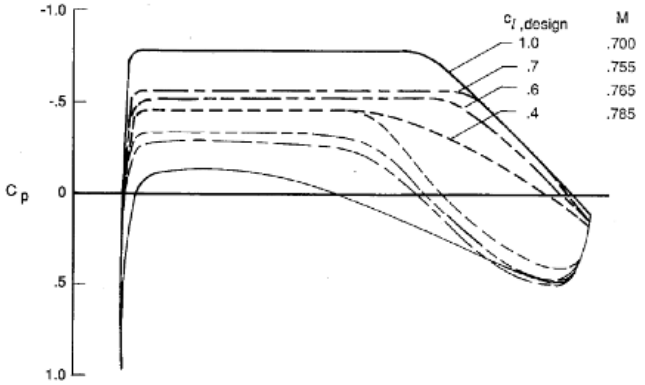

Fig. 2. 10% thickness SC(2) airfoil pressure coefficient distributions for various design lift coefficients.

value of the Mach number at which the sonic plateau (local Mach number of one) occurs. The sonic plateau for the 0.4 design lift coefficient airfoil occurs at 0.785, which is again approximately the cruise Mach number. The airfoil was configured on the wing with a leading edge sweep angle of 17 degrees. This results in an effective cruise Mach number of 0.75 which helps delay the effects of transonic flow. The wing planform and a summary of geometric and aerodynamics variables are shown in Fig. 3, including the cruise Reynolds number of 6.3×10^6 (based on mean aerodynamic chord) and an average lift-to-drag ratio of 23.55.

C. Fuselage Design

Considering the relatively high subsonic cruise speed, one of the fitst considerations for the fuselage design was a high fuselage length to diameter in order to reduce its form factor and thus the viscous drag. With this in mind, the overall dimensions of the fuselage were selected in order to properly accomodate the pilot and six passengers, baggage, fuel, and other supporting flight systems. A general idea of the shape of the fuselage is necessary in order to define the location and length of the main sections of the fuselage: the nose,

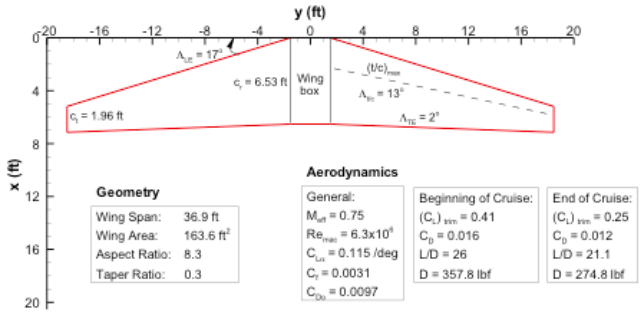

Fig. 3. Wing design summary of geometric and aerodynamic characteristics.

cockpit, cabin, and tail sections. In addition, an analytical expression is required to perform volumetric calculations to verify that the aircraft can satisfy flight requirements. Of most importance is to design the fuselage to hold sufficent fuel (in designated sections) for the intended mission and that the cabin is spacious enough for passengers. Finally, the shape is required from which to perform an aerodynamic analysis to estimate the drag particularly during cruise.

The fuselage design begins with an analytically definable shape and as it progresses through preliminary and detailed design, it is modified due to practical considerations. There are many general fuselage shapes, the shape for a particular design should be chosen based on type and purpose of the aircraft. We will select the shape known as a Sears-Haack, which is known to have relatively low wave drag compared to other shapes, and is an important consideration for transonic and supersonic aircraft. The curve for the top and botom walls of the fuselage is is described analytically as shown in Figure 4, where $r(x)$ is the local radius from the fuselage centerline at $z = 0$ at a given x location. The value of l is the length of the fuselage, which has been defined as 45 ft. A plot of the "P" exponent as a funtion of the nondimensional fuselage length, *x/L* is also shown in the figure. This exponent is a measure of the local curvature of the top and bottoms walls, i.e. a higher value corresponds to a sharper curvature such as observed in the tail.

The left and right wall of the fuselage (i.e. top view profile) are now defined utilizing the same Sears-Haack equation. The P distribution (same for both walls due to symmetry) is also shown in Fig. 5, notice that the value of P is zero when the fuselage wall is horizontal from x/L = 0.2 to 0.5. The size and shape of the fuselage has now been defined analytically, and the side and top profiles are shown in Fig. 6 and Fig. 7 respectively. Notice that the maximum height and width of the fuselage is 6.3 ft and 4.4 ft. Considering the average of these values (an average diameter of 5.35 ft) the length to diameter ratio is 8.41 ft. With this information, the surface area and volume of the fuselage can be calculated by considering 100 small fuselage cross section elements. The computed total surface area and volume are approximately 555 ft^2 and 638 ft^3. A summary of the fuselage aerodynamics in cruise conditions are shown in Fig. 6, most importantly a total drag of 278 lbf which was calculated utilizing an elemental fuselage drag approach. The skin friction value of 0.22 was

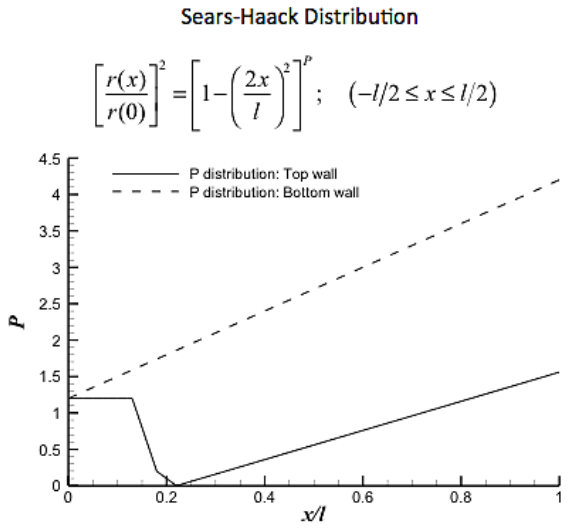

Fig. 4. P exponent distribution for the top and bottom fuselage walls.

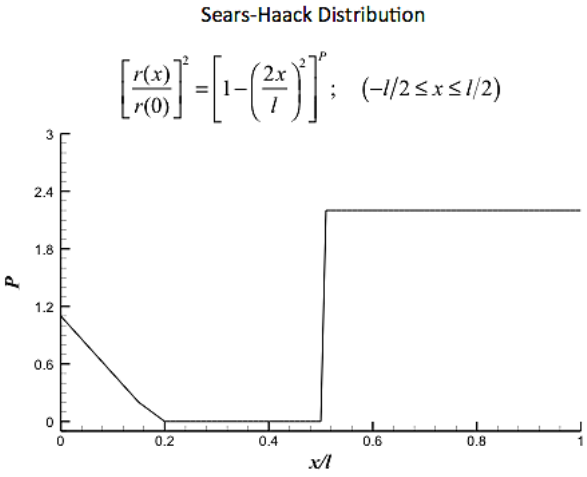

Fig. 5. P exponent distribution for the fuselage side walls.

calculated using the skin friction equation for turbulent flow on a flat plate, considering cruise Mach number and effective Reynolds number (as a function of x) with a roughness height, k of 2.08 for smooth paint.

D. Tail Design

The horizontal and vertical tail design deals with important conceptual design considerations such as the type of tail arrangement utilized, its size and placement on the fuselage. A "T-tail" configuration, which places the horizontal tail on top of the vertical tail, was selected as the ideal option. This configuration is not only the most popular for business jets, but compared to a conventional tail it has the following advantage: it allows for an effective reduction in size of both surfaces due to less wing downwash interaction (since the horizontal

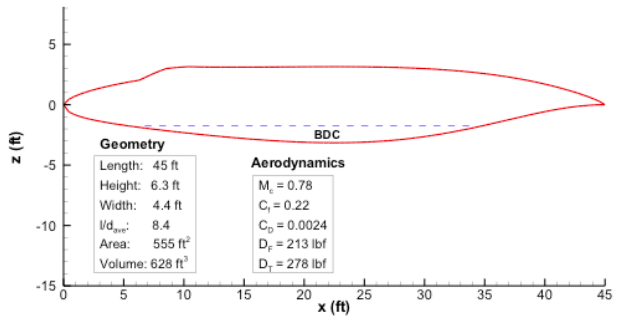

Fig. 6. Fuselage side profile and summary of aerodynamic characteristics.

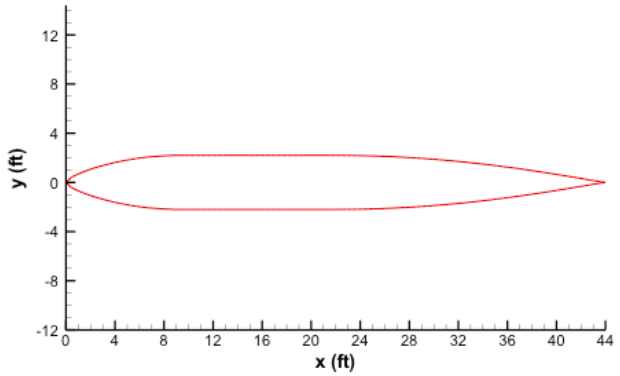

Fig. 7. Fuselage top profile.

tail is placed on top of the vertical tail) and it acts like a winglet for the vertical tail, thereby reducing induced drag. The vertical and horizontal tails were sized in terms of surface area according to a relation that considers the main wing span, the wing surface area, wing mean chord, the distance bethween the mean aerodynamic quarter-chord of the vertical/horizontal tails and wing. Finally, there is a vertical and horizontal tail coefficient that accounts for differences in tail surface area for a wide variety of aircraft types. Based on this criteria for business jets, values of 0.086 and 0.95 were utlized for the vertical and horizontal tail coefficients respectively.

The three most important considerations in selecting the tail airfoil were the following: (i) the need for a symmetric airfoil (zero theoretical lift production at zero degree angle of attack), (ii) a low base drag coefficient for cruise conditions, and (iii) a high critical Mach number (greater than the cruise Mach number). With these considerations, several candidate airfoils emerged: the NACA SC(2) 0010, NACA 0010-64, and NACA 64A-010. Ultimately, the NACA 0010-64 airfoil was deemed superior and selected based on a more optimal combination of zero-lift drag, lift-to-drag ratio, lift curve slope, and stall angle of attack.

With the tail surface area and airfoil charactersitics, the tail planform and aerodynamics analysis could be accomplished. The tail aspect ratios, taper ratios, and leading edge wing sweeps were chosen based on current business jet designs with similar cruise Mach numbers. The aerodynamic characteristics

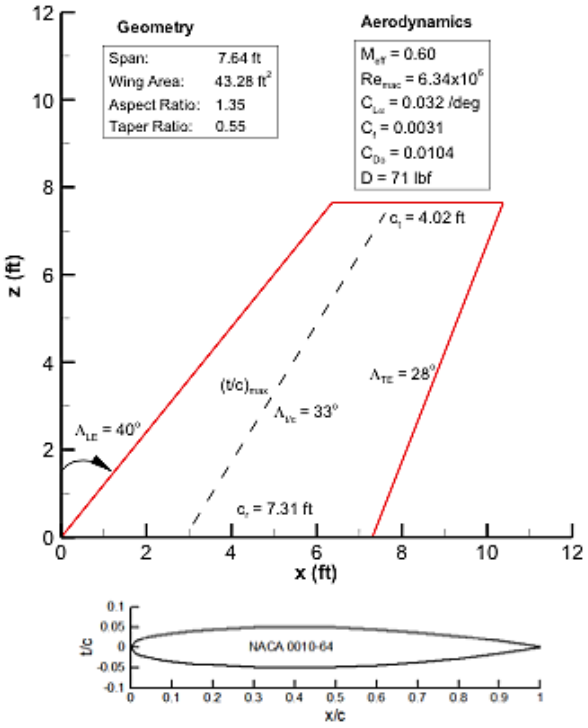

Fig. 8. Vertical tail geometric and aerodynamic characteristics.

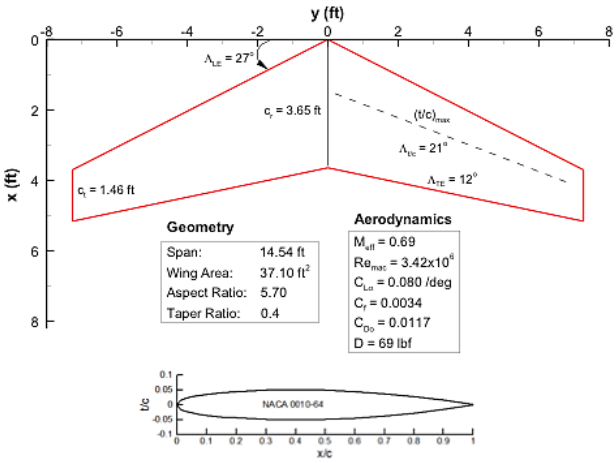

Fig. 9. Horizontal tail geometric and aerodynamic characteristics.

were computed based on analytical formulation similar to the wing. A summary of the vertical and horizontal tail geometry and aerodynamics are presented in Fig. 8 and Fig. 9. It was calculated that the vertical and horizontal tail produce about 71 lbf and 69 lbf of drag respectively.

E. Propulsion and Mission Analysis

The turbine engines are sized according to their ability to generate sustained thrust equal to or greater than the total drag in cruise. The thrust produced by turbofan engines decreases considerably with altitude, due to the effects of lower pressure,

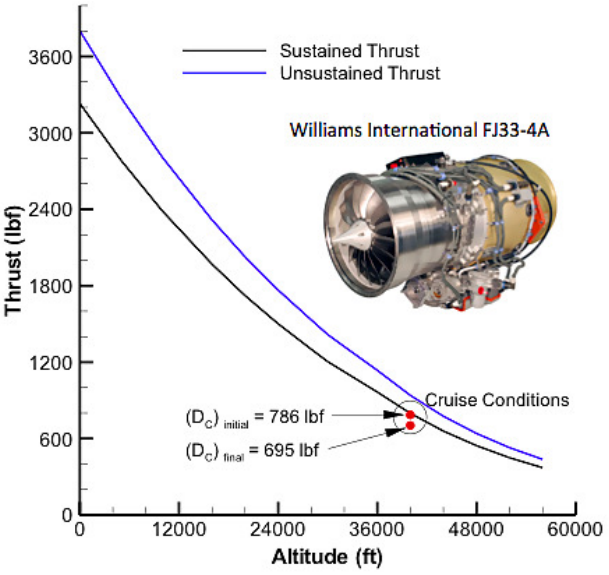

Fig. 10. WI FJ33-4A (2) combined thrust vs altitutde.

density, and temperature. Based on previous calculations of the component drag for the main wing, fuselage, and tail surfaces, the total generated cruise drag is 786 lbf at the beginning of cruise, and 695 lbf at the end of cruise (due to fuel expenditure and thus decreased lift and induced drag penalty). This signifies that the selected turbofan/s must be capable of producing a combined sustained thrust (about 85% of the maximum thrust) equal to or greater than 786 lbf. The generated thrust of a turbofan at a given altitude (in this case 40,000 ft) can be approximated given the thrust at sea level (provided by the engine manufacturer) and the pressure and temperature ratios, i.e. the pressure and temperature at that altitude normalized by the sea level pressure and temperature. Fig. 10 is the computed combined thrust as a function of altitude for a pair of Williams International FJ33-4A turbofan engines. This engine has a rating of 1,900 lbf maximum thrust and a specific fuel consumption of 0.486 lb/hr-lbf at sea level. Notice the sharp decrease in thrust with altitude; at the cruise altitude of 40,000 ft, the two engines produce a sustained thrust about equal to the aircraft drag at initial cruise.

With this thrust information, a *thrust-altitude-time* mision profile (thrust and altitude as a function of time) can be formulated and plotted. We will assume a mission with the maximum aircraft range of 3,300 nm. For the purpose of this analysis, the mission is composed of four phases: (i) take-off and climb, (ii) acceleration, (iii) cruise, and (iv) descent and landing. The time duration for each phase was calculated utilizing the known parameters; the cruise altitude, total range (distance), and engine thrust at a given altitude, and calculating the theoretical climb and descent rates. Based on this information, the thrust-altitude-time mission profile is given in Fig. 11. The entire mission duration is 7.68 hr, and the cruise phase accounts for 6.53 hr (traveling at 447 kn/hr) or 85% of the mission.

Each mission phase is described by an equation (relating

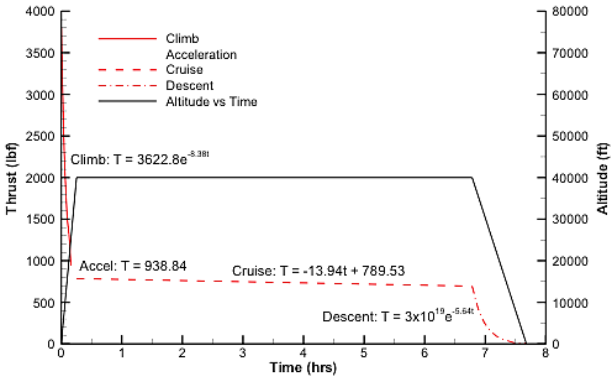

Fig. 11. Thrust-altitude-time mission profile.

$$\text{Climb: } \int_0^{0.16} 3622.8e^{-8.38t}\,dt = \left[-432.32e^{-8.38(0.16)}\right] - \left[-432.32e^{-8.38(0)}\right] = 319.21 \text{ hr-lbf}$$

$$\text{Acceleration: } \int_{0.16}^{0.253} 938.84\,dt = \left[938.84(0.253)\right] - \left[938.84(0.16)\right] = 87.31 \text{ hr-lbf}$$

$$\text{Cruise: } \int_{0.253}^{6.78} -13.94t + 789.53\,dt = \left[-6.97(6.78)^2 + 789.53(6.78)\right] - \left[-6.97(0.253)^2 + 789.53(0.253)\right] = 4{,}835.49 \text{ hr-lbf}$$

$$\text{Descent: } \int_{6.78}^{7.68} 3x10^{19}e^{-5.64t}\,dt = \left[-5.32x10^{18}e^{-5.64(7.68)}\right] - \left[-5.32x10^{18}e^{-5.64(6.78)}\right] = 132.06 \text{ hr-lbf}$$

Total Mission: 5,374 hr-lbf

Fig. 12. Integration of the time-thrust phase functions.

the thrust at a given time) and is labeled in Fig. 11. These equations can be integrated (with the lower and upper limit of integration corresponding to the time when the mission phase begins and ends) in order to compute the time-thrust expenditure of the engines in terms of hr-lbf. Fig. 12 shows a summary of the integration procedure leading to the following engine time-thrust expenditures: (i) takeoff and climb; 319.21 hr-lbf, (ii) acceleration; 87.31 hr-lbf, (iii) cruise; 4,835.49 hr-lbf, and (iv) descent and landing; 132.06 hr-lbf. An additional expenditure of 173.75 hr-lbf was alloted for loiter/fuel reserves, which brings the total design expenditure to 5,548 hr-lbf. These values can furthermore be utlized together with the *thrust specific fuel consumption* (TSFC) of the engines to calculate the amount of fuel required for the entire mission. Two values of TSFC for the selected turbofan engine were estimated based on sea level ratings given by the manufacturer. An estimated value of 0.64 lb/hr-lbf was utilized for climb and descent, and 0.8 lb/hr-lbf was used for acceleration and cruise. The fuel required for each phase was obtained by multiplying the engine time-thrust expenditure by TSFC, which resulted in the following pounds of fuel.

1) Climb: 205 lb
2) Acceleration: 70 lb
3) Cruise: 3,868 lb
4) Descent: 85 lb
5) Loiter/ fuel reserve: 112 lb

The total estimated fuel required for a maximum range 3,300 nm mission is thus about 4,340 lb of fuel, where the cruise phase requires about 89% of this total. Converting this value to gallons of fuel using a standard density of jet-fuel

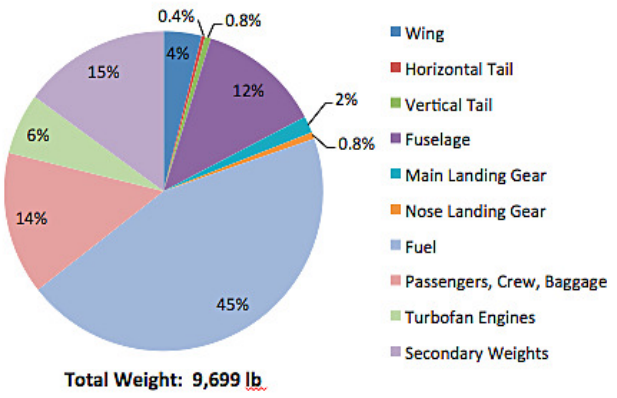

Fig. 13. Statistical primary component weights.

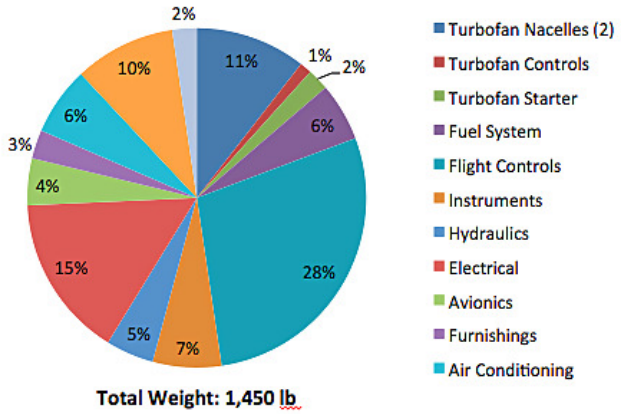

Fig. 14. Statistical secondary component weights.

of 6.76 lb/gal results in 642 gallons of fuel. Although not included in this discussion, analysis of the volume contained in a conceptual wing box and the below deck compartment of the fuselage indicated that this amount of fuel can be stored in multiple fuel tanks.

F. Statistical Weight Analysis

A statistical weight analysis was performed in order to more accurately estimate the takeoff weight of the TransAtlantic and determine the feasibility for under 10,000 pound takeoff weight. This method utilizes statistical equations based on regression analysis of commercial transport aircraft [14], [15]. The formulation is similar to that used by aircraft manufacturers during conceptual design. The primary component weights are given as: main wing, fuselage, vertical tail, horizontal tail, main landing gear, and nose landing gear. The pie chart of Fig. 13 shows the percentage weight of these components along with the total weight for secondary components. It is important to note that for the primary structural components, a composites matetial (CM) factor of 0.67 was applied to the equations. This signifies that through the use of carbon fiber and other composite materials, a theoretical weight reduction of 33% was achieved from traditional aircraft materials such as aluminum assumed in the equations. A reduction of up to 36% weight savings has been theorized using modern composites materials and fabrication techniques, so this assumption is realistic. Using this statistical weight analysis, a takeoff weight of 9,699 lb was calculated, which is below the 10,000 lb maximum. Notice that about 45% of the takeoff weight is due to fuel, and the secondary components makeup 15% of the total weight.

The secondary weights were also calculated using statistial equations for these components. A summary of these components are as follows: turbofan nacelles (2), turbofan controls, turbofan starter, fuel system, flight controls, instruments, hydraulics, electrical, avionics, and furnishings. Fig. 14 is a pie chart of the weight of these secondary components, where the total is about 1,450 lb. This statistical weight analysis gives a good preliminary estimate of the takeoff weight that indicate that such a design under 10,000 lb takeoff weight is feasible.

G. Structural Analysis

Acquiring a comprehensive calculation of the loads involved on the aircraft allows us to perform a structural analysis consisting of the shear and moment distribution along the wingspan and the fuselage longitudinal axis. First, the design load factor should be determined so that the aircraft materials and inner support strcuture can be designed to cope with these stresses. The maximum expected load factor should be calculated based on FAR-25 for commercial airplanes. This is given as an expression in terms of the takeoff weight. The maximum load factor is thus calculated as about 3.33. Using a recommended factor of safety of 1.5, this value is multiplied to arrive at the design load factor of 5.

The wing lift distribution is computed using an average of the trapezoidal and elliptical lift distribution. Here, the base lift, L is equal to the takeoff weight, the wingspan, b is 36.9 ft, and the taper ratio, λ is equal to 0.30. The main wing loads are as follows: the base lift (9,700 lb), flap lift (2,425 lb), wing weight (749 lb), and wing fuel (357 lb). These loads are distributed among the left and right wing half when computing lift per unit span, shear, and moment. Fig. 15 is a plot of the wing lift distribution, the wing and fuel weight, and the resultant wing load. This information is utilized to determine the combined shear and bending moment distribution using an elemental approach where half the wing is divided into 20 elements. We can observe in Fig. 16 that the maximum shear and moment of 5,959 lbf and 47,617 ft-lbf occur at the wing root as expected.

The shear and moment distributions for the fuselage is also determined in a similar elemental approach as the wing by dividing the fuselage into 20 elements and summing each component. Fig. 17 is a diagram of the fuselage loads (obtained from the statistical weight analysis) describing the magnitude and location of the loads. The shear force and bending moment were computed about the center of lift and plotted on Fig. 18. Notice that the location of maximum shear and moment is at about the CL which is the support and reaction force location. The CL location is not exact due to the

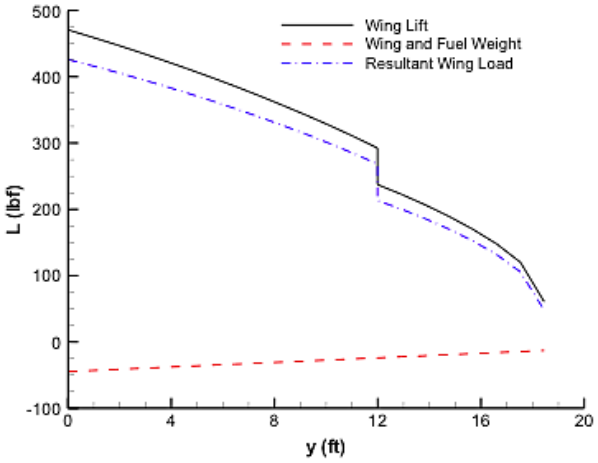

Fig. 15. Wing load distribution.

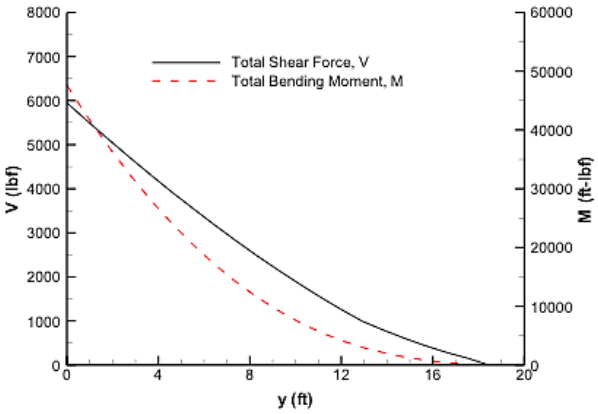

Fig. 16. Wing shear and moment distribution.

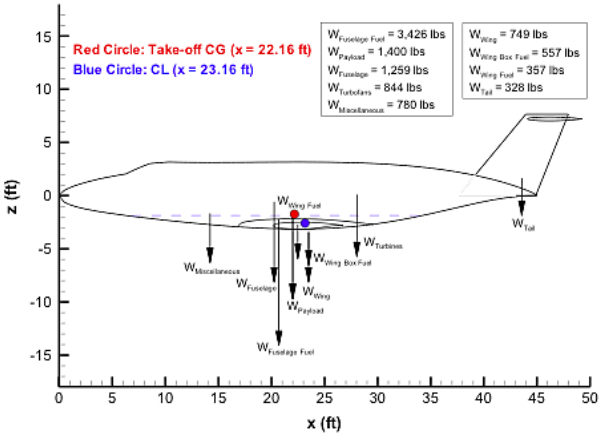

Fig. 17. Fuselage load distribution.

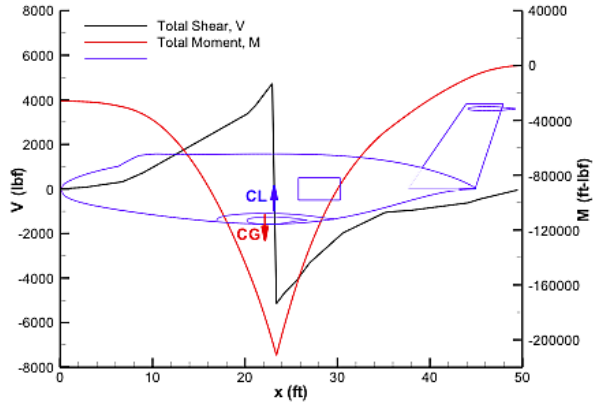

Fig. 18. Fuselage shear and moment distribution.

element of width $L/20$ not occuring at the precise location. The shear magnitude reaches 4,042 lbf and reverses sign after the reaction force at the CL. The shear force approaches zero at the nose and tail of the fuselage as expected. The moment distribution shows a similar behavior, where the maximum absolute moment of -38,200 ft-lbf is produced at about the CL. The moment also tends to zero at the nose and tail of the fuselage.

H. Loads and Static Stability

The complete array of component weights obtained in the statistical weight analysis will be applied to analyze the longitudinal stability and static margin of the aircraft. A positive longitudinal static stability exhibits a nose-down pitching moment after a disturbance. This is caused by the center of gravity (CG) lying ahead of the center of lift (CL). Fig. 19 shows the magnitude and normalized fuselage location of the loads. A summation of the loads and moments created reveal that the CG lies at a distance of 22.59 ft from the nose. On the other hand, the CL is located approximately 23.18 ft, just behind the CG. The pitch-down moment created about the CL is calculated as -5,377 ft-lb, and the lift that must be generated by the horizontal tail in order to create a positive moment to counteract this moment is -227 lbf.

The static margin (SM) of the aircraft gives an indication of the longitudinal stability, or tendency for the nose of the aircraft to return to a neutral position. The SM is defined as the x location of the CL minus the x location of the CG quantity divided by the mean aerodynamic wing chord of 4.65 ft. The SM is thus equivalent to about 0.119, which yields positive static stability and is representative of the value halfway through the cruise phase. Fig. 20 is a plot of the SM as a function of time from takeoff to landing for a 3,300 nm mission. As the aircraft burns fuel, the CG shifts closer to the CL, thus decreasing the SM. As shown in the figure, the SM decreases from about 21.6% at takeoff to 5.95% at landing without loitering. The coefficient of longitudinal stability, C_{M_α} was calculated by multiplying the negative of the SM (0.119) by the lift curve slope, C_{L_α} of the main wing. This results in a value for C_{M_α} of -0.785/rad, which represents positive stability typical of commercial jets at high subsonic Mach

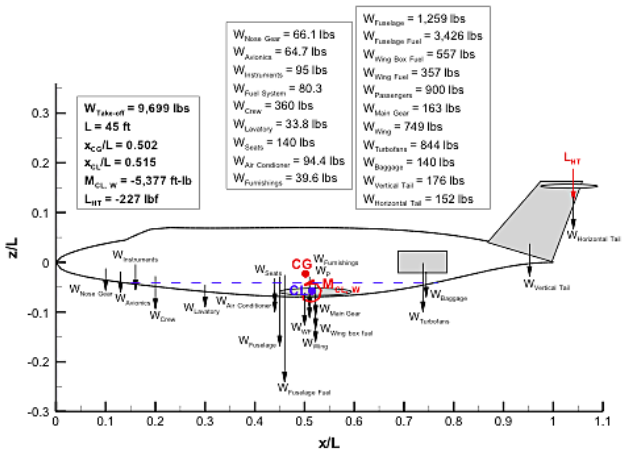

Fig. 19. Component loads and location for longitudinal static stability.

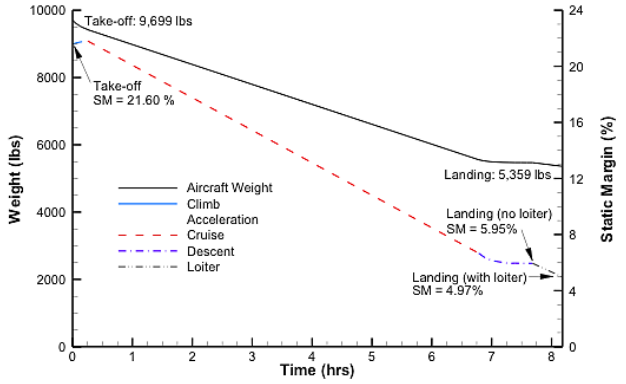

Fig. 20. Static margin as a function of time for a 3,300 nm mission.

numbers.

The coefficients of directional, C_{n_β} and lateral stability, C_{l_β} of the aircraft were also calculated using analytical calculations that consider directional stability influences by the wing, fuselage, and vertical tail. The formulation is approximate, as there are many factors that affect directional and lateral stability, however the calculation gave values of 0.131/rad for C_{n_β} and -0.131/rad for C_{l_β} (which is approximated as the negative of the directional stability coefficient due to a lack of a more accurate analytical expression) at this stage of conceptual design.

I. Conceptual Design Conclusions

The main objective of the conceptual design process presented thus far was to develop an aircraft configuration with a set of design requirements and provide preliminary analysis that supports feasibility for transatlantic range under 10,000 lb takeoff weight. All the major phases of conceptual design have been covered to a basic level such that any main component or subsystem can be developed futher into preliminary design or for research purposes. Moreover, the conceptual design at this stage does not necessarily represent

Fig. 21. TransAtlantic conceptual design CAD model.

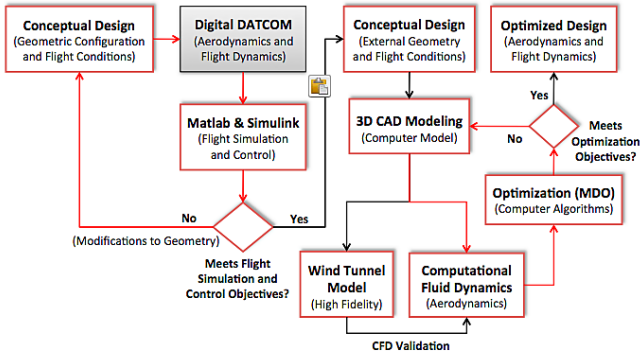

Fig. 22. Preliminary design process flowchart.

an advancement in fuel-efficiency design over existing aircraft, rather it is intended as a research platform where novel aerospace technology (leading to weight reduction, propulsion efficiency, and drag reduction) or methodologies can be applied and integrated to existing design characteristics such that some aspect of performance can be increased to reduce fuel expenditure and CO_2 emissions standards.

The conceptual design geometry was modeled in the Unigraphics computer aided deisgn (CAD) software and a rendered view is shown in Fig. 21. One important reason for developing CAD drawings is to utilize them as inputs to generate a mesh for computational fluid dynamics (CFD) simulation. CFD analysis is a critical component of the preliminary design process. Preliminary design of aircraft is a process to refine the aircraft design utilizing more advanced analysis methods and computational approaches. This process requires specialized knowledge in different fields related to the aircraft system and is often performed in separate development teams and later integrated. Such refined analysis methods were applied with regards to the aerodynamic and flight dynamics control design of the TransAtlantic. The process flowchart for development on aerodynamic design, flight dynamics and control, and optimization is illustrated in Fig. 22.

These methods shown as process blocks are part of ongoing investigations outside the scope of this paper, however the flowchart can explained as follows. The conceptual design geometry is imputed into the shaded gray box labeled “Digital DATCOM.” Digital DATCOM is a program orginally

developed by the Air Force and McDonell Douglas in the 1970's for conceptual design analysis and has since become an open-source design tool with community support. This program computes the static and dynamic derivatives from an input file with the aircraft geometric and flight parameters. The flowchart shows how this information can be imputed into Matlab/ Simulink to perform a simulation and study the flight dynamic behavior of the aircraft. If the required simulation objectives are met, a 3D CAD model is created to rapid prototype a wind tunnel model and prepare a CFD model for testing and simulation for high-fidelity analysis. The last step in the process is optimization of the CFD model via simulations to achieve some desired aerodynamic performance objectives. The resulting aircraft geometry is considered an "optimized" design and concludes the preliminary design portion of the aerodynamics and flight dynamics and control of the TransAtlantic.

III. Application of Active Flow Control as a "Green" Aircraft Technology

The TransAtlantic aircraft design serves as a research platform for the application of advanced or "green" aircraft technologies. As an example, details of the aircraft (such as the wing) can be reproduced into a physical sub-scale prototype for integration of a new technology and testing inside a wind tunnel. Active flow control is a subfield of fluid dynamics that aims to improve the aerodynamic performance of a body subject to airflow. It is is generally applied as a technique to modify the airflow around the body, thus having an effect on the pressure and shear stress distributions, and consequently the lift and drag. Recent relevant studies on active flow control have focused on control of flow separation on airfoils [16], sub-scale flight and wind tunnel scale aircraft models [17], and the feasibility of implementing this technology on civil transport aircraft [18]. There are various types of actuators to modify the airflow, here we are concerned with fluidic actuators which inject a synthetic jet across the body surfarce into the boundary layer. In this scenario, the selective application of synthetic jets (at ideal locations on the airfoil and for a range of post-stall angles of attack) increase the momentum of the boundary layer causing the flow to reattach. This type of actuator and flow performance enhancement was observed in the author's wind tunnel studies on airfoil sections of wind turbine blade models [19], [20]. However, the limitation of these actuators when using piezoelectric disks as the driving diaphragm, is the very small momentum transfer compared to the momentum of the flow over the airfoil section (on the order of 10^{-3}). Thus, most applications of this technique have been demonstrated in wind tunnels for Reynolds numbers that are considered laminar flow in most cases.

The implementation of synthetic jet-based flow control techniques for full-scale aerodynamic systems (with Reynolds numbers in the millions) such as manned aircraft has not be demonstrated. The two major challenges is signficiantly increasing the momentum created by the synthetic jet actuator (as mentioned earlier) and developing a robust actuator that

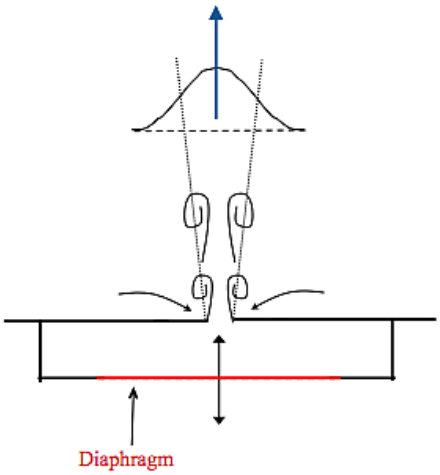

Fig. 23. Synthetic jet actuator schematic.

can function in the adverse environmental conditions of flight. A unique actuator that greatly improves the first criteria of increasing momentum transfer is currently in development by the author. It is referred to as an *electromagnetic synthetic jet* (EMSJ) actuator. This actuator uses a strong alternating magnetic field input (generated via current through coils of copper wire) to drive a magnetic diaphragm. This results in 2-3 orders of magnitude larger diaphragm amplitude displacements (compared to piezoelectric materials), and thus the ability to excite a much larger volume of air leading to a higher momentum jet. A general schematic of a synthetic jet actuator is shown in Fig. 23 as described in the study by Glezer [21]. The diaphragm can be either piezoelectric or magnetic, but it functions in the same manner. As it resonates at high frequencies inside of a cavity, it ingests the surrounding air and expells it back out through an orifice where the jet is synthesized. The actuator is characterized as zero-net-mass flux (though momentum is transfered) and mechanically simple and low cost.

If the challenges to creating a robust high-momentum synthetic jet actuator can be overcome, they may be integrated on manned aircraft wings and horizontal/ vertical tail surfaces. Such actuators may have the potential to replace control surfaces such as ailerons and reduce the weight of hydraulic systems. By manipulating the lift (through circulation control at the trailing edge of the airfoil) along the span of the wing, you can generate a net moment that may be able to roll the aircraft, thus achieving flight control. A general procedure to continuing development of the EMSJ actuator for aircraft (as a form of advanced "green" aircraft technology) is summarized as follows:

1) Initiate an extensive EMSJ actuator development program following a *CPOI* process; characterization, parameterization, optimization, and integration of the actuator.
2) Integration and testing of EMSJ actuators into a 1/6th scale TransAtlantic half-wing wind tunnel model.
3) Integration and testing of a 1/6th scale TransAtlantic

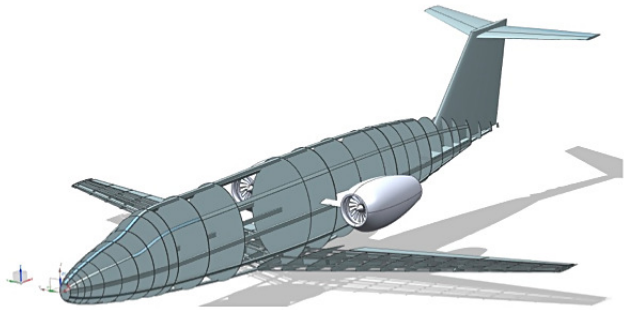

Fig. 24. 1/6 scale TransAtlantic flight demonstrator.

flight demonstrator to establish flight performance with and without EMSJ actuators.

The last step involves integrating the novel active flow control system on the wings of a 1/6th scale remotely piloted model of the TranAtlantic and measuring the flight dynamics (particularly the roll performance such as with an inertial measurement unit). The flight demonstrator will achieve a maximum flow Reynolds number (based on mean aerodynamic wing chord) of about 1 million. Thereafter, the active flow control system will be applied on progressively larger sub-scale aircraft, and eventually to full-scale manned civil aircraft through university and industry partners with this capability. Figure 24 is a CAD assembly of the airframe structure of the flight demonstrator; the structural components have been designed, yet the aircraft has not been manufactured. The goal is to fligh-test the demonstrator with two wing structures; a baseline wing (as shown integrated in the figure) and an active flow control wing with the actuators embedded on the wing.

IV. Conclusion

This paper discusses the conceptual design details of the TranAtlantic; a "green" aircraft design that is intended as a research platform for the application of advanced technology or methods that can be utilized to increase fuel efficiency and reduction in CO_2 emissions over existing aircraft. The aircraft was designed and analyzed using "first-order" analytical formulation typical of the conceptual design process. The overall geometry and dimensions of the aircraft were established, and the design was modeled in CAD using the Unigraphics software. Of particular interest to the author is exploring how active flow control can be applied as a "green" technology on a scale model of the TransAtlantic to contribute to the aerodynamic efficiency of aircraft. To this end, a research plan was proposed which includes: (i) development of a novel and more powerful electromagnetic synthetic jet actuator, (ii) integration and testing of these actuators on a 1/6 scale half-wing model of the TransAtlantic inside a wind tunnel, and (iii) integration and flight-testing of a 1/6 scale TransAtlantic flight demonstrator to evaluate the performance of the active flow control technology for distributed lift and flight control. One of the main goals of this research initiative is to attract national and international researchers in other fields related to aerospace to advance the state-of-the-art in propulsions, structures, etc. and contribute to more sustainable commercial air travel.

Acknowledgment

The author would like to acknowledge the various graduate and undergraduate students who have contributed to the design and analysis of the TransAtlantic. In particular, Souma Chowdhury and Jie Zhang for the response surface analysis of the aircraft lift-to-drag ratio to main geometric design variables. Thanks to Jason Li for solid modeling of the aircraft and development of CAD drawings for the full-scale geometry and flight demonstrator structure.

References

[1] *Green Growth and the Future of Aviation*, 27th Round Table on Sustainable Development, 2012.
[2] *Green Aviation: A Better Way to Treat the Planet*, NASA, 2010.
[3] E. Kronenberg and J. White, *The Future of Green Aviation*, Booz and Allen Inc., 2008.
[4] *Clean Sky at a Glance*, Clean Sky JU, www.cleansky.eu, Belgium, 2013.
[5] *NextGen*, Federal Aviation Administration, www.faa.gov/nextgen, 2014.
[6] *Environmentally Responsible Aviation Project*, NASA, http://www.aeronautics.nasa.gov/isrp/era/htm, 2014.
[7] B. Boling, L. Bortner, E. Hendricks, and D. Mavris, "Designing for a Green Future: A Unified Aircraft Design Methodology," *Journal of Aircraft*, vol.47, no. 5, 2010.
[8] K. Franz, K. Risse, and E. Stumpf, "Framework for Sustainability-Driven Aircraft Design," AIAA Aviation Technology, Integration, and Operations Conference, Los Angeles, CA, August 12-14, 2013.
[9] T.I. Saeed and W.R. Graham, "Conceptual Design for a Laminar-Flying-Wing Aircraft," 50th AIAA Aerospace Sciences Meeting, Nashville, TN, January 09-12, 2012.
[10] D. P. Raymer, *Aircraft Design: A Conceptual Approach*, 4th ed., American Institute of Aeronautics and Astronautics, 2006.
[11] T. C. Corke, *Design of Aircraft*, 1st ed., Prentice Hall, 2002.
[12] A. K. Kundu, *Aircraft Design*, Cambridge University Press, 2010.
[13] C. D. Harris, "NASA Supercritical Airfoils," Langley Research Center, Hampton, VA, NASA Tech. Paper 2969, 1990.
[14] R. Staton, "Cargo/ Transport Statistical Weight Estimation Equations," Vought Aircraft Rep. 2-59320/8R-50475, 1968.
[15] A. Jackson, "Preliminary Design Weight Estimation Program, "AeroCommander Division, Rep. 511-009, 1971.
[16] N. O. Packard, M. P. Thake, C. H. Bonilla, K. Gompertz, and J. P. Bons, "Active Control of Flow Separation on a Laminar Airfoil," *AIAA Journal*, vol. 51, no. 5, 2013.
[17] R. King, N. Heinz, M. Bauer, T. Grund, and W. Nitsche, "Flight and Wind-Tunnel Tests of Closed-Loop Active Flow Control," *Journal of Aircraft*, vol. 50, no. 5, 2013.
[18] M. Jabbal, S. C. Liddle, and W. J. Crowther, "Active Flow control Systems Architecture for Civil Transport Aircraft," *Journal of Aircraft*, vol. 47, no. 6, 2010.
[19] V. Maldonado, M. Boucher, R. Ostman, and M. Amitay, "Active Vibration Control of a Wind Turbine Blade Using Synthetic Jets, *International Journal of Flow Control*, vol. 1, no. 4, 2010.
[20] V. Maldonado, J. Farnsworth, W. Gressick, and M. Amitay, "Active Control of Flow Separation and Structural Vibrations of Wind Turbine Blades, *Wind Energy*, vol. 13, pp. 221-237, 2010.
[21] A. Glezer and M. Amitay, "Synthetic Jets," *Ann. Rev. of Fluid Mech.*, vol. 34, pp. 503-529, 2002.

Victor Maldonado Victor Maldonado is an Assistant Professor in the Department of Mechanical Engineering at the University of Texas at San Antonio since the Fall of 2013. Prior to that, he was a Postdoctoral Research Associate at the National Wind Resource Center at Texas Tech University. He completed his B.S. and Ph.D. in Aerospace Engineering from Rensselaer Polytechnic Institute in 2004 and 2012 respectively. Dr. Maldonados research interests and expertise focuses on the synthesis of methodologies in active flow control, aerodynamics, flight dynamics/ control, and design into complex systems such as aircraft and wind turbines.